Research Square

Preprints are preliminary reports that have not undergone peer review.
They should not be considered conclusive, used to inform clinical practice,
or referenced by the media as validated information.

J84-Coded Interstitial Lung Disease Co-Certification in U.S. Deaths Attributed to Intracerebral or Subarachnoid Hemorrhage, 1999–2024: a Serial Cross-Sectional Study

Christina Cacoulidis

ccynb@ymsystem.edu

University of Missouri–Kansas City School of Medicine

Travis Homan

St. Luke's Hospital

Research Article

Keywords: interstitial lung disease, pulmonary fibrosis, intracerebral hemorrhage, subarachnoid hemorrhage, mortality, CDC WONDER, epidemiology

Posted Date: November 16th, 2026

DOI: https://doi.org/10.21203/rs.3.rs-11310894/v1

License: This work is licensed under a Creative Commons Attribution 4.0 International License.
Read Full License

Additional Declarations: No competing interests reported.

Abstract

Background

National death-certificate co-certification of J84-coded interstitial lung disease (ILD) with deaths attributed to intracerebral hemorrhage (ICH) or subarachnoid hemorrhage (SAH) has not been characterized. We quantified this coding-defined intersection in the United States.

Methods

We performed a serial cross-sectional analysis of CDC WONDER Multiple Cause of Death data for 1999–2024. Deaths were included when I60 or I61 was the underlying cause and J84 was listed as a multiple cause. Primary estimands were the aggregate co-certification proportion and hemorrhage-subtype distribution. A 95% Wilson confidence interval was calculated for the overall co-certification proportion. Segmented Poisson modeling was limited to the complete combined J84 series; series with suppressed annual cells were not trend-modeled because suppression is informative.

Results

Among 604,331 U.S. deaths attributed to SAH or ICH, 551 carried J84, an aggregate co-certification proportion of 0.091% (95% CI, 0.084%–0.099%); 437 were ICH and 114 were SAH. The combined crude population mortality rate was 0.050 per 1,000,000 in 1999 and 0.100 in 2024. A secondary exploratory model of the complete combined J84 series selected a 2012 change point, but this model used the U.S. population rather than annual fatal SAH/ICH deaths as its denominator. J84.1 accounted for 410 co-certified deaths (74.4%); its annual trend was not modeled because the 2009 cell was suppressed. SAH-specific, sex-interaction, and exact COVID-exclusion trends were not estimable.

Conclusions

J84-coded ILD was rarely co-certified among deaths attributed to SAH or ICH. These data provide a national surveillance baseline with a precisely estimated but very small aggregate co-certification proportion. Secondary crude population-rate trends do not measure annual ILD representation among fatal hemorrhagic-stroke deaths, and subgroup trends with suppressed years were not estimated.

Background

Nontraumatic intracerebral hemorrhage (ICH) and subarachnoid hemorrhage (SAH) are high-fatality cerebrovascular emergencies whose management often requires intensive cardiopulmonary support [1–3]. Interstitial lung diseases (ILDs) are heterogeneous parenchymal disorders that can impair gas exchange and, in advanced disease, contribute to pulmonary vascular and right-heart dysfunction [4, 5].

ILD is therefore a plausible marker of limited physiologic reserve in neurocritical illness, but biologic plausibility does not establish a hemorrhagic-stroke-specific association.

Existing evidence is sparse and indirect. Population studies of idiopathic pulmonary fibrosis (IPF) have described vascular comorbidity, and U.S. claims data have documented intracranial hemorrhage among patients with IPF [8–10]. These observations establish coexistence but do not show that ILD is overrepresented among fatal ICH or SAH deaths or that it modifies survival. Death-certificate surveillance can quantify co-certification at population scale, but a multiple-cause code does not encode temporal sequence, disease severity, treatment exposure, or causal contribution.

Temporal interpretation is further complicated because national J84-coded mortality and certification practices have changed during the ICD-10 era, including during the COVID-19 pandemic [6, 7]. A rise in deaths carrying both hemorrhagic-stroke and J84 codes could therefore reflect changes in pulmonary disease burden, diagnostic recognition, death-certificate coding, hemorrhagic-stroke mortality, or several of these factors.

We used 26 years of U.S. multiple-cause mortality data to quantify how often J84-coded ILD was co-certified when SAH or ICH was the underlying cause of death. The primary objective was to estimate the aggregate co-certification burden and its distribution by hemorrhage subtype. Secondary analyses described population mortality over time, examined a narrower J84.1 coding definition, and summarized demographic patterns where disclosure rules permitted valid estimation. Co-certification was treated as a surveillance phenotype rather than as a patient-level exposure, risk factor, or causal contributor.

Methods

Study design and data source

We designed a retrospective, serial cross-sectional study using the CDC WONDER Multiple Cause of Death database. CDC WONDER compiles death-certificate data from the 50 U.S. states and the District of Columbia. Each record includes a single underlying cause of death and up to 20 additional multiple causes, together with demographic information [11, 12]. Beginning in 1999, mortality causes are coded using the International Classification of Diseases, Tenth Revision (ICD-10) [13].

To cover the full 1999–2024 interval without double counting the overlapping years available in the two contemporary WONDER data families, we prespecified use of the Multiple Cause of Death 1999–2020 bridged-race database for 1999–2017 and the Multiple Cause of Death 2018–2024 single-race database for 2018–2024. This nonoverlapping approach has been used in recent 1999–2024 cerebrovascular mortality studies and prevents duplicate inclusion of deaths from 2018–2020 [14].

Case definition

The primary cohort included U.S. resident deaths for which nontraumatic SAH (ICD-10 I60) or nontraumatic ICH (I61) was recorded as the underlying cause of death and a J84-category interstitial pulmonary disease was recorded as a multiple cause. The pulmonary co-certification variable is described as “J84-coded ILD” rather than all ILD because clinically important ILDs coded outside J84, including sarcoidosis (D86), hypersensitivity pneumonitis (J67), and some connective-tissue-disease-associated ILDs, are not comprehensively captured by this code family [6, 7].

SAH and ICH were analyzed separately and in a combined hemorrhagic-stroke cohort. The primary pulmonary definition included the J84 category. A prespecified sensitivity analysis restricted the pulmonary phenotype to J84.1, “other interstitial pulmonary diseases with fibrosis.” This narrower definition was used as a coding-restriction check rather than as a gold-standard clinical definition of fibrotic ILD.

Outcomes and stratification

The analysis was organized around distinct estimands to avoid denominator conflation (Table 1). Primary descriptive measures were the total number of deaths meeting the joint SAH/ICH–J84 definition, the aggregate proportion of all I60/I61 underlying-cause deaths carrying J84 as a multiple cause, and the distribution of co-certified deaths between ICH and SAH. The overall aggregate proportion was accompanied by a 95% Wilson score confidence interval. Annual crude population mortality rates were secondary measures of national burden. Age-adjusted mortality rates (AAMRs), standardized to the 2000 U.S. population and expressed per 1,000,000 persons, were used only when CDC WONDER designated them reliable. Population-rate trends were not interpreted as annual co-certification prevalence among fatal SAH/ICH deaths.

Table 1
Study definitions and estimands

Component	Primary definition / estimand	Secondary / sensitivity definition	Interpretive role
Data period	1999–2017 D77 + 2018–2024 D157	—	Uses nonoverlapping WONDER eras and avoids duplicate 2018–2020 records
Hemorrhage phenotype	Underlying cause I60 (SAH) or I61 (ICH)	Separate ICH and SAH descriptions	Restricts cohort to deaths attributed to nontraumatic intracranial hemorrhage
Pulmonary phenotype	J84 listed as a multiple cause	J84.1, other interstitial pulmonary diseases with fibrosis	Administrative co-certification definitions, not adjudicated clinical ILD
Primary estimand	Aggregate proportion of I60/I61 underlying-cause deaths carrying J84, with 95% Wilson CI	Distribution of co-certified deaths by hemorrhage subtype	Measures co-certification among fatal hemorrhagic-stroke deaths
Secondary temporal measure	Annual crude population mortality; reliable AAMRs when available	Segmented Poisson model for complete combined J84 series only	Measures population burden, not annual co-certification proportion
Pandemic sensitivity	All eligible deaths	J84 + U07.1 co-certification in 2020–2024	Exact exclusion was not estimable because cells were suppressed
Suppressed annual cells	Not reconstructed	No formal trend coefficient for affected series	Avoids informative-missingness bias and preserves CDC disclosure rules

Prespecified demographic analyses examined sex and age. Age-specific results were summarized for 45–64, 65–74, 75–84, and ≥ 85 years where exact aggregation was possible. Race/ethnicity analyses were not pooled because bridged-race and single-race classifications differ and the already sparse joint phenotype would have generated extensive additional suppression.

Statistical analysis

CDC WONDER supplied counts, population denominators, crude rates, AAMRs, and 95% confidence intervals. Counts of 9 or fewer and their associated rates were suppressed, and CDC WONDER designates rates based on fewer than 20 deaths as unreliable. Suppressed values were retained as “Suppressed,” were not displayed numerically, and were not reconstructed by subtraction or imputation. Rates flagged “Unreliable” by WONDER were not treated as quantitative AAMR outcomes. Because suppression identifies small counts rather than random missingness, annual series containing suppressed cells were not used for inferential trend models.

The complete combined J84 series was examined secondarily with log-linear segmented Poisson regression of annual deaths using log population as an offset. Continuous linear splines with zero to three candidate change points and a minimum four-year segment length were compared by Bayesian information criterion (BIC). Segment slopes were transformed to annual percent change (APC), and average annual percent change (AAPC) represented the interval-weighted average log slope. Wald confidence intervals are conditional on the selected Poisson model, assume the fitted Poisson variance structure, and do not account for breakpoint-selection uncertainty. With only 26 annual observations, these estimates were treated as descriptive rather than confirmatory; no breakpoint was interpreted as a validated epidemiologic threshold.

Annual ICH, SAH, sex-specific, J84.1, and COVID-excluded series contained suppressed cells and therefore were not assigned formal trend coefficients. Planned year-by-hemorrhage-type and year-by-sex interaction models likewise required reportable annual counts for both levels and were not estimable.

Two sensitivity analyses were prespecified. First, the pulmonary phenotype was restricted to J84.1-coded other interstitial pulmonary diseases with fibrosis and summarized using aggregate counts and reportable annual rates. Because the 2009 J84.1 cell was suppressed, no full-period trend coefficient was estimated without imputing or otherwise reconstructing a protected small cell. Second, 2020–2024 deaths were queried for simultaneous J84 and U07.1 co-certification. All annual J84-plus-U07.1 cells and the aggregate five-year count were suppressed, preventing exact COVID-excluded estimates without impermissible reconstruction.

Use of generative artificial intelligence

ChatGPT (OpenAI) was used during manuscript preparation to assist with language editing, organization, and journal-formatting. The authors are responsible for the final manuscript.

Reporting

Reporting followed the Strengthening the Reporting of Observational Studies in Epidemiology (STROBE) framework [15]. CDC WONDER data-use restrictions were followed throughout.

Results

Overall national mortality burden

Across 1999–2024, 604,331 U.S. deaths had I60 or I61 recorded as the underlying cause. Of these, 551 also carried a J84 multiple-cause code, corresponding to an aggregate co-certification proportion of 0.091% (95% Wilson CI, 0.084%–0.099%). ICH accounted for 437 co-certified deaths (79.3%) and SAH for 114 (20.7%); the corresponding aggregate co-certification proportions were 0.096% for ICH and 0.076%

for SAH (Table 2). These unadjusted subtype proportions summarize the full 26-year period and should not be interpreted as subtype-specific risk estimates.

Table 2
Co-certification burden and secondary population mortality, 1999–2024

Group	Deaths, n	Aggregate co-certification proportion	1999 crude rate*	2024 crude rate*	AAPC, % (95% CI)
SAH + J84	114	0.076%	Suppressed	0.029	Not estimable
ICH + J84	437	0.096%	0.043	0.071	Not estimated‡
SAH/ICH + J84	551	0.091% (95% CI, 0.084%–0.099%)	0.050	0.100	1.6 (0.5 to 2.7)

*Rates are per 1,000,000 U.S. population. The aggregate co-certification proportion for the combined SAH/ICH + J84 cohort was 0.091% (95% Wilson CI, 0.084%–0.099%). AAPC for the combined series is a secondary exploratory population-rate measure and does not represent an annual J84 co-certification proportion among fatal SAH/ICH deaths. Model-based intervals are conditional on the selected Poisson model. ‡The ICH annual series contained a suppressed 2009 cell; no trend coefficient was reported because suppression is informative.

The combined crude population mortality rate was 0.050 per 1,000,000 (14 deaths) in 1999 and 0.100 per 1,000,000 (34 deaths) in 2024. The 2024 AAMR was 0.087 (95% CI, 0.062–0.121); the 1999 AAMR was designated unreliable and was not used for direct age-adjusted comparison. In the complete combined J84 series, BIC selected one change point at 2012: the crude population mortality rate declined during 1999–2012 (APC, − 3.0%; 95% CI, − 5.4% to − 0.5%) and increased during 2012–2024 (APC, 6.8%; 95% CI, 4.2%–9.5%); full-period AAPC was 1.6% (95% CI, 0.5%–2.7%) (Fig. 1; Table 2). These estimates describe crude population mortality involving both conditions, not the annual probability that a fatal SAH/ICH death carried J84.

Intracerebral versus subarachnoid hemorrhage

ICH accounted for the larger absolute number of co-certified deaths (437 vs 114) and had a higher unadjusted aggregate co-certification proportion (0.096% vs 0.076%). Formal annual subtype trends were not estimated because the ICH series contained a suppressed 2009 cell and SAH cells were suppressed for all years in 1999–2017 and five of seven years in 2018–2024. Because suppression is informative and the subtype populations differ substantially in age and clinical profile, these aggregate differences do not establish greater susceptibility to co-certified ILD in ICH.

Sex and age patterns

Women accounted for 291 co-certified deaths and men for 260. Crude population rates were 0.071 per 1,000,000 person-years among women and 0.065 among men, whereas era-specific age-adjusted rates were descriptively higher in men (0.060 vs 0.043 in 1999–2017 and 0.076 vs 0.059 in 2018–2024)

(Table 3). Because crude and age-adjusted comparisons differed and annual sex-specific cells were frequently suppressed, no sex effect was inferred. Adults aged ≥ 85 years had the highest reportable age-specific rates (0.893 per 1,000,000 in 1999–2017 and 1.403 in 2018–2024), followed by those aged 75–84 years (0.558 and 0.671, respectively). Age 45–64 results were not consistently reportable under suppression constraints.

Table 3
Descriptive sex and age patterns

Stratum	Co-certified deaths, n	Crude / age-specific rate	Era-specific AAMR	Interpretation
Female	291	0.071†	0.043 / 0.059	Crude and age-adjusted ordering differed; no sex effect inferred
Male	260	0.065†	0.060 / 0.076	Crude and age-adjusted ordering differed; no sex effect inferred
Age 65–74	—	0.168 / 0.185	Not applicable	Age-specific rate by 1999–2017 / 2018–2024 era
Age 75–84	—	0.558 / 0.671	Not applicable	Age-specific rate by 1999–2017 / 2018–2024 era
Age ≥ 85	—	0.893 / 1.403	Not applicable	Highest observed age-specific rates
Age 45–64	—	Not consistently reportable	Not applicable	Suppression limited consistent era-specific reporting

†Pooled sex-specific crude population rates; age-specific rates are shown separately for 1999–2017 and 2018–2024 because denominators were extracted by database era. Rates are per 1,000,000.

Sensitivity analyses

Restricting the pulmonary phenotype to J84.1-coded other interstitial pulmonary diseases with fibrosis identified 410 deaths (74.4% of the broad J84 cohort), including 333 ICH and 77 SAH deaths (Fig. 2; Table 4). The 2009 J84.1 annual count was suppressed. Because that missingness directly denotes a small protected count, no full-period J84.1 trend coefficient was estimated. For 2020–2024, all annual J84-plus-U07.1 counts and the aggregate five-year count were suppressed, so exact COVID-excluded rates and slopes were not estimable.

Table 4
Coding-definition and suppression-limited sensitivity analyses

Analysis	Group	Deaths, n	Trend estimate	Interpretation
J84.1 restriction	Combined	410	Not estimated*	2009 annual cell suppressed; aggregate burden reported
J84.1 restriction	ICH	333	Not estimated	Suppressed annual cell(s); descriptive count only
J84.1 restriction	SAH	77	Not estimated	Extensive suppression
COVID-19 exclusion	Combined	Suppressed	Not estimable	All J84 + U07.1 cells were suppressed

*No full-period J84.1 trend coefficient was estimated because the 2009 annual count was suppressed. CDC suppression identifies a small count and is therefore informative missingness; the protected value was neither reconstructed nor imputed.

Discussion

This national death-certificate study establishes that J84-coded ILD is rarely co-certified when SAH or ICH is recorded as the underlying cause of death: 551 of 604,331 deaths, or 0.091% (95% CI, 0.084%–0.099%), over 26 years. The principal contribution is this denominator-anchored surveillance estimate and the explicit separation of aggregate co-certification from crude population mortality. ICH comprised most co-certified deaths, but neither the larger count nor the modestly higher unadjusted aggregate proportion can be interpreted as a subtype-specific risk difference without adjustment for the very different populations in which ICH and SAH occur.

The temporal analysis is secondary. In the complete broad-J84 series, crude population mortality declined before a model-selected 2012 breakpoint and increased thereafter. This trajectory is not an annual co-certification proportion, is not age adjusted, and may reflect population aging, changes in overall ILD mortality, diagnostic recognition, death-certificate practice, hemorrhagic-stroke mortality, or several of these factors. Recent national ILD surveillance likewise demonstrates secular change in J84-coded mortality, reinforcing the need to avoid interpreting the joint crude-rate pattern as hemorrhagic-stroke specific [6, 7].

The J84.1 restriction provides a descriptive coding-definition check rather than an inferential comparison. J84.1 represented 74.4% of broad-J84 co-certified deaths, but its 2009 annual cell was suppressed. Because suppressed cells are known to be small, dropping the year would create informative missingness and could bias a fitted slope. We therefore report the aggregate J84.1 burden and annual pattern graphically without assigning a formal full-period trend coefficient. This avoids implying that a trend estimated only from reportable years is unbiased.

Suppression materially shaped the estimable questions. SAH-specific and ICH-specific temporal trends, a year-by-sex interaction, the J84.1 full-period slope, and exact COVID-excluded analyses could not be estimated without either excluding informative low-count years or reconstructing protected cells. The decision not to do so preserves CDC disclosure rules and avoids presenting potentially biased subgroup slopes. Demographic patterns remain descriptive because crude and age-adjusted sex comparisons differed and several age-specific cells were not consistently reportable.

Clinical interaction between chronic parenchymal lung disease and severe brain injury remains plausible but untested here. The appropriate next step is denominator-matched, patient-level validation using adjudicated ILD subtype and severity, pulmonary physiology, hemorrhage severity, treatment intensity, ventilation course, withdrawal-of-life-sustaining-therapy decisions, case fatality, and functional outcome after ICH or SAH.

Limitations

First, death-certificate codes are not clinically adjudicated diagnoses. J84 is heterogeneous, does not capture every ILD phenotype, and may incompletely record chronic comorbidity on the death certificate. The 0.091% estimate is therefore a certification proportion, not the prevalence of ILD among people who die from hemorrhagic stroke. J84.1 is narrower but is not a gold-standard definition of fibrotic ILD, and diagnostic recognition or certification practice may have changed over 26 years.

Second, J84 recorded as a multiple cause does not establish temporal sequence, disease severity, or causal contribution and provides no pulmonary function, imaging pattern, oxygen requirement, smoking history, antithrombotic exposure, hemorrhage volume, aneurysm status, neurologic examination, procedural treatment, hospital capability, or withdrawal-of-life-sustaining-therapy information. Patient-level confounding and treatment selection therefore cannot be addressed.

Third, the joint phenotype was sparse. Most annual AAMRs and many subgroup cells were unreliable or suppressed. Suppression is informative because it identifies small counts; excluding suppressed years can bias annual trend estimates, which is why subgroup trend models were not reported. The complete combined temporal analysis relied on crude population rates because reliable annual AAMRs were unavailable and therefore cannot separate population aging from other secular changes. Breakpoint selection searched several candidate segmented models using only 26 annual observations; model-based intervals assume the fitted Poisson variance structure and do not include model-selection uncertainty. The temporal model also used the U.S. population rather than annual I60/I61 deaths as its denominator, so it cannot determine whether the yearly co-certification proportion changed. Finally, the mortality design cannot estimate ILD prevalence among living hemorrhagic-stroke patients, hemorrhage incidence in ILD, case fatality, treatment efficacy, or causal effects.

Conclusions

Within the limitations of this dentiform bench-top study, the tested static surgical-guide workflow produced mean absolute axial depth and angular deviations of 0.369 mm and 1.864° across 42 implant positions. CT-to-surface comparison yielded a mean case-level residual standard deviation of 0.235 mm across 28 model-region cases. The exploratory analysis in five matched models did not establish a statistically significant association between registration metrics and placement outcomes. These findings characterize the tested workflow and do not establish clinical safety, effectiveness, or superiority.

Abbreviations

AAPC, average annual percentage change

AAMR, age-adjusted mortality rate

APC, annual percentage change

BIC, Bayesian information criterion

CDC, Centers for Disease Control and Prevention

CI, confidence interval

ICD-10, International Classification of Diseases, Tenth Revision

ICH, intracerebral hemorrhage

ILD, interstitial lung disease

IPF, idiopathic pulmonary fibrosis

SAH, subarachnoid hemorrhage

STROBE, Strengthening the Reporting of Observational Studies in Epidemiology

WONDER, Wide-ranging Online Data for Epidemiologic Research

Declarations

Ethics approval and consent to participate

This study analyzed publicly available, deidentified, aggregate mortality data from CDC WONDER and involved no direct participant contact or identifiable private information. Institutional review board approval and informed consent were therefore not required for this analysis of publicly available aggregate data.

Consent for publication

Not applicable.

Availability of data and materials

The datasets analyzed during the current study are publicly available through the CDC WONDER Multiple Cause of Death database (https://wonder.cdc.gov/mcd.html). Derived analytic data and statistical code are available from the corresponding author on reasonable request, subject to CDC WONDER data-use restrictions and preservation of suppression labels.

Competing interests

The authors declare that they have no competing interests.

Funding

No specific funding was received for this study.

Authors' contributions

CC conceived the study, developed the methodology, performed the investigation, curated and analyzed the data, prepared the visualizations, and drafted and revised the manuscript. TH provided clinical supervision, contributed to interpretation of the pulmonary findings, and critically revised the manuscript. Both authors read and approved the final manuscript.

Acknowledgements

Not applicable.

References

1. Palaniappan LP, Allen NB, Almarzooq ZI, et al. Circulation. 2026;153(9):e275–906. 10.1161/CIR.0000000000001412. 2026 Heart Disease and Stroke Statistics: A Report of US and Global Data From the American Heart Association.
2. Greenberg SM, Ziai WC, Cordonnier C, et al. 2022 Guideline for the Management of Patients With Spontaneous Intracerebral Hemorrhage: A Guideline From the American Heart

Association/American Stroke Association. Stroke. 2022;53(7):e282–361. 10.1161/STR.0000000000000407.

3. Hoh BL, Ko NU, Amin-Hanjani S, et al. 2023 Guideline for the Management of Patients With Aneurysmal Subarachnoid Hemorrhage: A Guideline From the American Heart Association/American Stroke Association. Stroke. 2023;54(7):e314–70. 10.1161/STR.0000000000000436.
4. Raghu G, Remy-Jardin M, Richeldi L, et al. Idiopathic Pulmonary Fibrosis (an Update) and Progressive Pulmonary Fibrosis in Adults: An Official ATS/ERS/JRS/ALAT Clinical Practice Guideline. Am J Respir Crit Care Med. 2022;205(9):e18–47. 10.1164/rccm.202202-0399ST.
5. Panagiotou M, Church AC, Johnson MK, Peacock AJ. Pulmonary vascular and cardiac impairment in interstitial lung disease. Eur Respir Rev. 2017;26(143):160053. 10.1183/16000617.0053-2016.
6. Grover P, Jain R, Kaur G, Singh B. Interstitial Lung Disease in the United States: CDC Mortality Trends (1999–2024). Adv Respir Med. 2026;94(4):51. 10.3390/arm94040051.
7. Leary C, Bine C, Baral N, Bin Abdul Jabbar A, Mirza A, Mirza M, et al. Trends in interstitial lung disease and the COVID-19 pandemic in the United States from 1999 to 2022. Respir Res. 2025;26(1):277. 10.1186/s12931-025-03350-2.
8. Hubbard RB, Smith C, Le Jeune I, Gribbin J, Fogarty AW. The association between idiopathic pulmonary fibrosis and vascular disease: a population-based study. Am J Respir Crit Care Med. 2008;178(12):1257–61. PMID:18755924.
9. Dalleywater W, Powell HA, Hubbard RB, Navaratnam V. Risk factors for cardiovascular disease in people with idiopathic pulmonary fibrosis: a population-based study. Chest. 2015;147(1):150–6. PMID:25121965.
10. Nathan SD, Basavaraj A, Reichner C, et al. Characterizing Health Outcomes in Idiopathic Pulmonary Fibrosis using US Health Claims Data. Respiration. 2021;100:108–18. PMCID:PMC7949201.
11. Centers for Disease Control and Prevention, National Center for Health Statistics. Multiple Cause of Death Data on CDC WONDER. https://wonder.cdc.gov/mcd.html. Accessed 7 Sep 2026.
12. Centers for Disease Control and Prevention, National Center for Health Statistics. Multiple Cause of Death 1999–2020: dataset documentation. https://wonder.cdc.gov/wonder/help/mcd.html. Accessed 7 Sep 2026.
13. Centers for Disease Control and Prevention, National Center for Health Statistics. Instructions for Classifying Multiple Causes of Death, 2024. https://www.cdc.gov/nchs/nvss/manuals/2024/2b-2024.htm. Accessed 7 Sep 2026.
14. John A, Azhar F, Wasay A, et al. A quarter-century mortality analysis of concomitant infective endocarditis and stroke in the United States: a nationwide CDC WONDER study. J Stroke Cerebrovasc Dis. 2026;35(9):108720. 10.1016/j.jstrokecerebrovasdis.2026.108720.
15. von Elm E, Altman DG, Egger M, Pocock SJ, Gøtzsche PC, Vandenbroucke JP, STROBE Initiative. The Strengthening the Reporting of Observational Studies in Epidemiology (STROBE) statement:

guidelines for reporting observational studies. BMJ. 2007;335(7624):806–8. 10.1136/bmj.39335.541782.AD.

Figures

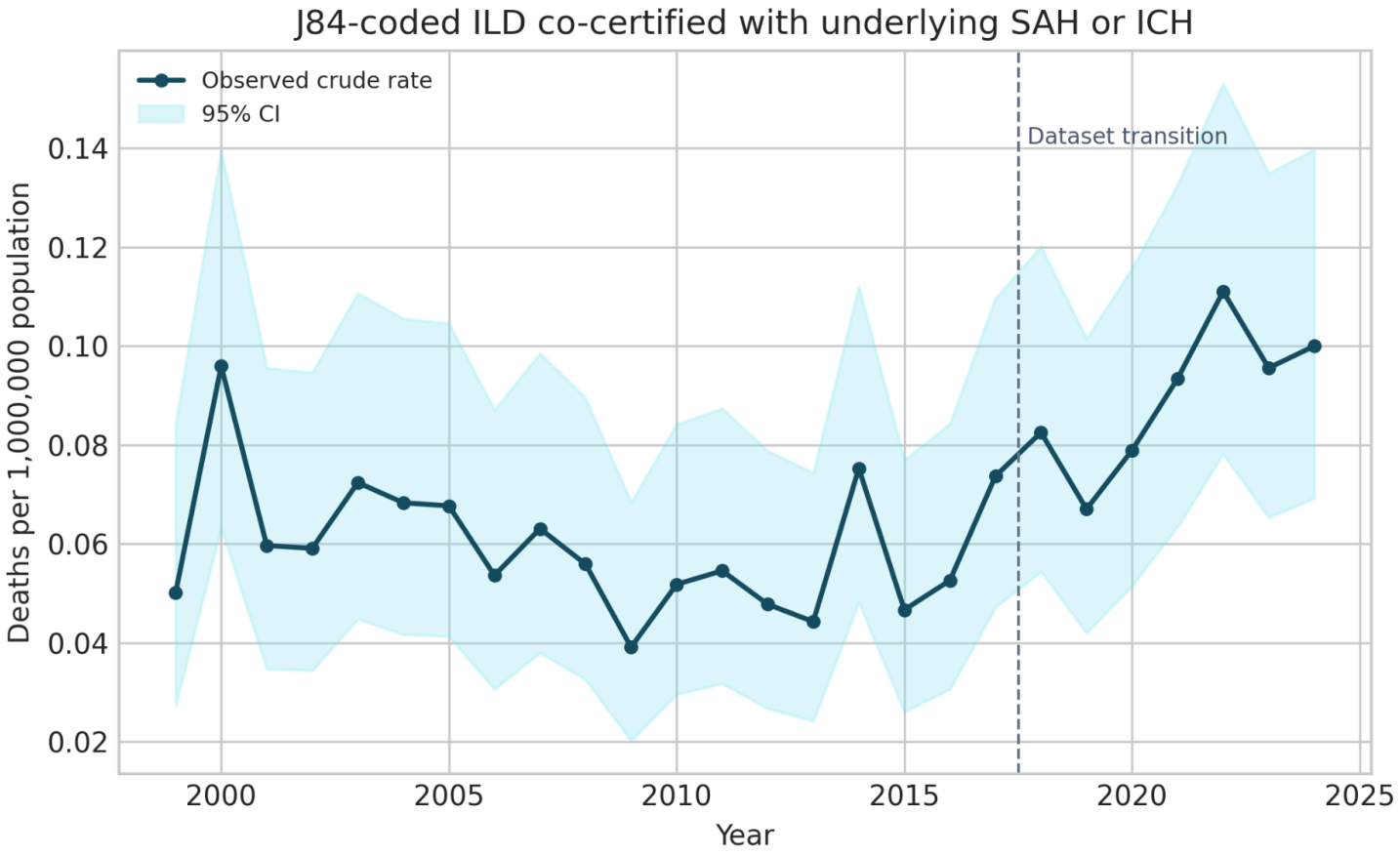


Figure 1

National population mortality involving hemorrhagic stroke and J84-coded ILD, 1999–2024. Points show annual crude population mortality rates for deaths with I60 or I61 as the underlying cause and J84 as a multiple cause; shading shows exact Poisson 95% confidence intervals. The fitted segmented trend is secondary and exploratory. It uses the U.S. population, not annual fatal SAH/ICH deaths, as the denominator and therefore does not measure the annual J84 co-certification proportion among fatal hemorrhagic-stroke deaths. The dashed line marks the transition between the nonoverlapping D77 and D157 data series.

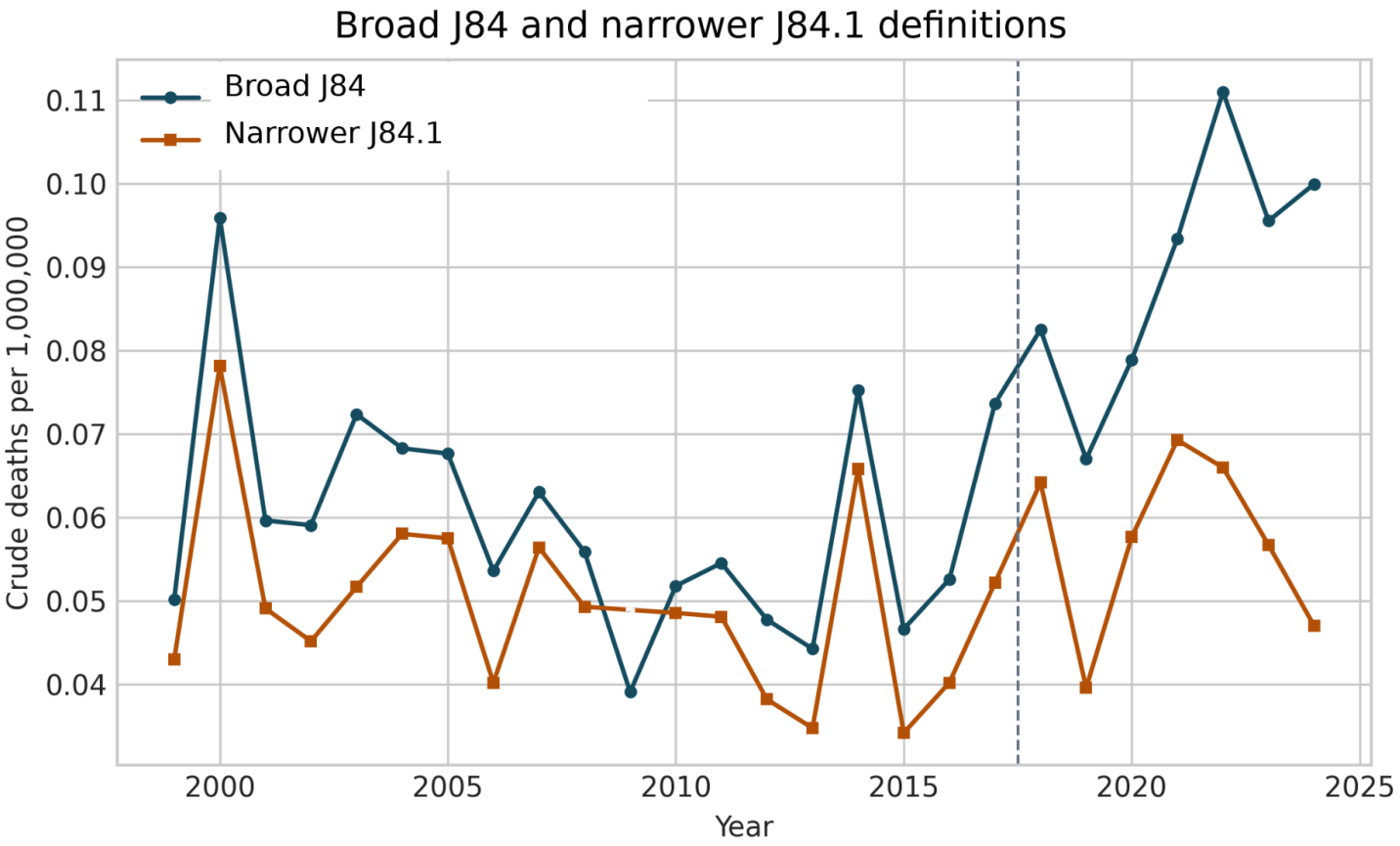


Figure 2

Broad J84 and J84.1 coding-definition sensitivity analysis. Annual crude population mortality rates are shown descriptively for the broad J84 definition and J84.1-coded other interstitial pulmonary diseases with fibrosis. The missing 2009 J84.1 value reflects CDC suppression and was neither reconstructed nor imputed. J84.1 is a narrower administrative coding definition, not a clinically adjudicated fibrotic-ILD phenotype. The dashed line marks the transition between the nonoverlapping D77 and D157 data series.